

Supplementary

I. Determining the crystallographic orientation of nanodiamond by HR-TEM

Much confusion can arise when attempting to determine the crystallographic orientation of nanodiamonds using SAED due to the large number of differently oriented particles contributing to the reflections. HR-TEM allows for the direct observation of the crystal's lattice spacing and is moreover not restricted by the selection rules imposed by the crystal's symmetry. The lattice spacings observed in both SAED and HR-TEM correspond to crystallographic planes perpendicular to the beam direction and thus the orientation of the crystal surface, but only if the (reasonable) assumption is made that nanodiamonds are deposited to lie flat on the TEM grid's surface. Under this assumption, crystal orientations that are not perpendicular to the observed spacings are ruled out.

Total no. of HR imaged ND's: 31			Observation (frequency)	
hkl	d (Å)	d ⁻¹ (nm ⁻¹)	SAED	HR real space
100	3.57	2.80	N.A.	1
111	2.06	4.85	+	30
200	1.79	5.60	N.A.	2
220	1.26	7.92	+	9
311	1.08	9.29	+	-
222	1.03	9.70	+	-
400	0.89	11.20	+	-
331	0.82	12.21	+	-
420	0.80	12.53	+/- (weak)	-
422	0.73	13.72	+	-
333 / 511	0.69	14.56	+	-
440	0.63	15.85	+/- (weak)	-
531	0.60	16.57	+/- (weak)	-
442 / 600	0.59	16.80	-	-

Table S1: Summary of the observed lattice spacings in the diffraction pattern (see figure 2a and 2b of the main text). Calculated lattice spacings based on a lattice constant $a = 3.57$ Å. N.A. = Not Allowed, i.e. symmetry forbidden. Total number of nanodiamonds with confirmed (110) orientation: 11.

For particles for which two lattice spacings were simultaneously observable, the orientation of the face was determined by taking the cross product of the scattering vectors. In 11 cases, the (110) could be confirmed this way. No observations were made of nanodiamonds with a confirmed orientation other than (110). In cases where only one spacing was observable, the observed spacing corresponded to the (111) family of planes in most cases, ruling out a similar (111) or (100) surface orientation as these directions are not perpendicular.

II. Calculation of T_1 and T_2 decoherence times

As can be derived from the Redfield theory ^{1,2}, the dependence of T_1 on fluctuating magnetic fields by a bath of spins is given by:

Equation 1.

$$\frac{1}{T_1} = \frac{1}{T_{1,bulk}} + 3\gamma_e^2 \langle B_{\perp}^2 \rangle \frac{\tau_c}{1 + \omega_0^2 \tau_c^2}$$

In the limit of short correlation times ($\tau_c \ll T_2$) T_2 is expressed as

Equation 2.

$$\frac{1}{T_2} = \frac{1}{T_{2,bulk}} + \frac{1}{2T_1} + \gamma_e^2 \langle B_{\parallel}^2 \rangle$$

With $\langle B_{\perp}^2 \rangle$ and $\langle B_{\parallel}^2 \rangle$ being the variance in the magnetic field directed perpendicular and parallel to the NV's quantization axis respectively, γ_e the electron's gyromagnetic ratio and $\omega_0 = 2\pi D$ with $D = 2.87 \text{ GHz}$ the ESR frequency of the NV center.

In above equations, the relaxation rates for nanodiamond are assumed to be the same as in bulk diamond ($T_{1,bulk}^{-1}$) except for the addition of relaxation through interaction with surface spins. Furthermore, the fluctuations of the spin bath are assumed to originate solely from intrabath dipolar coupling, leading to an expression for the correlation time of the spin bath τ_c :

Equation 3.

$$\frac{1}{\tau_c} = \frac{\mu_0 \gamma_e^2 \hbar C_S}{4r_{min}^2} \sqrt{\frac{2\sigma}{\pi}}$$

Where $C_S = \frac{1}{3}S(S+1)$, r_{min} the minimum distance between the surface bath spin and σ is the spin surface density. We considered a bath of $S = 1/2$ spins with parameters $r_{min} = 1.5 \text{ \AA}$ the nearest neighbor distance in diamond and $\sigma = 1 \text{ nm}^{-2}$ ³⁻⁵.

The dependence on shape and size of the particle is contained in the expressions for $\langle B_{\perp}^2 \rangle$ and $\langle B_{\parallel}^2 \rangle$:

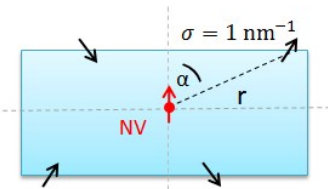


Figure 4: 2D cross section of diamond model

Equation 4.

$$\langle B_{\perp}^2 \rangle = \left(\frac{\mu_0 \gamma_e \hbar}{4\pi} \right)^2 C_S \sigma \oint_S \frac{(2 + 3\sin^2 \alpha(\theta, \phi))}{|\vec{r}|^6} dS \quad \text{a)}$$

$$\langle B_{\parallel}^2 \rangle = \left(\frac{\mu_0 \gamma_e \hbar}{4\pi} \right)^2 C_S \sigma \oint_S \frac{(1 + 3\cos^2 \alpha(\theta, \phi))}{|\vec{r}|^6} dS \quad \text{b)}$$

Where \vec{r} is the distance vector from the NV center to the bath spin and $\alpha(\theta, \phi)$ is the angle between \vec{r} and the NV's quantization axis, as indicated in figure 4. The values for $T_{1,bulk}$ and $T_{2,bulk}$ were chosen in accordance with experimental findings: $T_{1,bulk} = 3 \text{ ms}$ ^{3,6} and $T_{1,bulk} = 3 \text{ \mu s}$ ⁷⁻⁹.

Bibliography

- ¹ Slichter, C.P. *The Principles of Magnetic Resonance*, 3rd ed. (Springer, 1996).
- ² Redfield, A.G. *IBM J. Res. Dev.* **1**, 19 (1957).
- ³ Tetienne, J.P. *et al. Phys. Rev. B* **87**, 235436 (2013).
- ⁴ Tisler, J. *et al. ACS Nano* **3**, 1959 (2009).
- ⁵ Song, X. *et al. AIP Adv.* **4**, 0 (2014).
- ⁶ Jarmola, A. *Phys. Rev. Lett.* **108**, 1 (2012).
- ⁷ De Lange, G. *et al, Sci. Rep.* **2**, 382 (2012).
- ⁸ De Lange, G. *et al. Science* **330**, 60 (2010).
- ⁹ Hanson, R. *Phys. Rev. B* **74**, 161203 (2006).